Microstructural Representation and Transformation of Petroleum Coke via Self-Developed HRTEM Analytic Technique

Zihan You[1], Jin Xiao[2], Liuzhou Zhou[3], Yu Zhou[4] and Qifan Zhong[5]
1. Doctoral Candidate
2. Professor & Executive Deputy Director
3, 4. Doctoral Candidates
5. Professor & Carbon Laboratory Director
School of Metallurgy and Environment, Central South University & National Engineering Research Center of Low-carbon Nonferrous Metallurgy, Changsha, China
Corresponding author: zhongqifanchina@csu.edu.cn
https://doi.org/10.71659/icsoba2025-el005

Abstract

Carbon electrodes for aluminium electrolysis are mainly made of petroleum coke (PC, accounting for 85 wt.%). The amorphous phase of PC poses a challenge for the precise microstructure analysis, thus hindering the development of carbon electrode preparation processes. In recent work, we developed an intelligent lattice fringe extraction technique for amorphous carbon materials based on high-resolution transmission electron micrographs (HRTEM) detection and image binarization. The microstructural arrangement state and data (lattice length, orientation, curvature, stacking, etc.) of green petroleum coke (GPC) and calcined petroleum coke (CPC) were obtained via this integrated HRTEM analytic technique. Then the atomistic representations of GPC and CPC incorporating actual parameters were constructed for comprehensive observation and simulation via an automated modelling strategy. Furthermore, the microstructural transformation pattern of GPC across the industrial calcination temperature range (25 to 1600 °C) was explored and quantified based on a series of microstructural data at discrete temperature stages.

Keywords: Petroleum Coke, HRTEM, Lattice Fringe, Microstructural Analysis, Atomistic Modeling.

1. Introduction

Petroleum coke (PC) is the primary raw material for carbon electrodes in aluminum electrolysis cells, accounting for over 85 wt.% of the electrode composition [1]. PC is categorized as an amorphous carbon material with a complex microstructure characterized by the intertwining of sp2 and sp3 hybridized carbon atoms, diverse ONS functional group configurations, and the presence of hydrogen bonds [2]. Previous research has yet to provide an in-depth exploration of such intricate microstructural characteristics.

During the preparation of carbon electrodes, green petroleum coke (GPC) undergoes a calcination process to form calcined petroleum coke (CPC). This process involves pyrolysis, polymerization, and reordering of the carbon structure [2]. However, the precise mechanisms governing the microstructural evolution during calcination remain largely unexplored, representing a significant research gap. Consequently, in industrial production, extensive manual adjustments of equipment parameters are often required to accommodate the variations in GPC properties. It poses a bottleneck to the intelligent manufacturing of metallurgical carbon materials and the broader aluminum electrolysis sector. Addressing this bottleneck necessitates not only the precise characterization of PC microstructural features at the atomic scale but also a comprehensive understanding of the structural evolution across multiple calcination temperature stages.

Recent advances in the analysis of carbon network chains (aromatic layers) in amorphous carbon materials such as coal have provided new insights into the structural characteristics of such systems. Mathews et al. [3–5] employed the Materials Studio software platform in conjunction with high-resolution transmission electron microscopy (HRTEM) and Perl scripts such as Fring3D and Vol3D to achieve automated modeling of coal, coke, and carbon black. Louw et al. [6, 7] developed the Stack software based on Matlab, enabling quantitative analysis of aromatic layer stacking configurations by controlling center-to-center distance, nearest neighbor distance, and angular orientation. This approach allows the extraction of secondary, tertiary, quaternary, and quinary stacking configurations, facilitating subsequent data processing and calculation. Furthermore, Changan Wang et al. [8] investigated the curvature properties of aromatic layers in amorphous carbon materials using the Curvature script based on Matlab, segmenting the lattice fringes based on length and angular parameters to analyze directional layer curvature. Simultaneously, Huang Yang [9] et al. developed Perl scripts such as Cross_link.pl to connect aromatic layers and optimize the structural configuration of curved aromatic layers in activated carbon.

In this study, we integrated these advanced HRTEM-based methodologies to develop a comprehensive and intelligent lattice fringe extraction technique for carbon materials, allowing for a detailed characterization of the microstructural features of both PC and CPC. Additionally, we designed a customized Packmol script [10] to construct a multi-scale and visualizable model that effectively captures the microstructural characteristics and composition of PC and CPC. Furthermore, we investigated the evolution of PC microstructures, including lattice fringe length, stacking, orientation, and curvature, across various calcination temperature stages. The proposed intelligent lattice fringe extraction technique and the associated findings provide a solid theoretical foundation for the intelligent manufacturing of metallurgical carbon materials.

2. Methods

2.1 Coke Sample

The components of GPC samples used in this work are shown in Table 1, Cokes 1, 2 and 3 being respectively produced in Shandong Province, in Zhejiang Province, and at Tianjin Municipality, China. The samples were ground and sieved, with the −106 μm fraction selected for calcination. Approximately 70 g of dried powder was weighed for each batch and placed into a graphite crucible, which was then positioned at the center bottom of an alumina crucible. The remaining space in the alumina crucible was filled with landfill material to provide an oxygen-isolated environment during calcination. The samples were held at a setting temperature for 4 h to complete the calcination process. The setting temperature is in the range from 298 to 1873 K. The heating rate was set at 5 K/min below 1273 K and 3 K/min above 1273 K. The furnace model used was KSL-1700X, manufactured by Hefei Kejing Materials Technology Co., Ltd.

Table 1. Ultimate analyses of green petroleum coke samples (wt.%).

Samples	C	H	N	S	O
Coke 1	89.53	3.38	1.27	2.45	2.27
Coke 2	89.08	3.55	1.37	2.67	3.33
Coke 3	86.47	3.46	1.77	4.19	4.11

2.2 HRTEM Analytic Technique

The HRTEM Analytic Technique for carbon materials involves HRTEM detections in combination with a suite of software tools and scripts. The methodology is outlined in detail below, in the order of usage (Figure 1), platform compatibility, and underlying principles.

HRTEM detections were conducted at the Advanced Research Center, Central South University, using a Tecnai G2F20 field-emission transmission electron microscope (FEI, USA). The sample was crushed into a fine powder using a quartz mortar for approximately 30 minutes, dried for 2 hours, and then dispersed in ethanol. After ultrasonic treatment in a bath for 20 minutes, the suspension was drop-cast onto a copper grid. The microscope has a point resolution of 0.24 nm and a line resolution of 0.102 nm, with an accelerating voltage range of (20–200) kV.

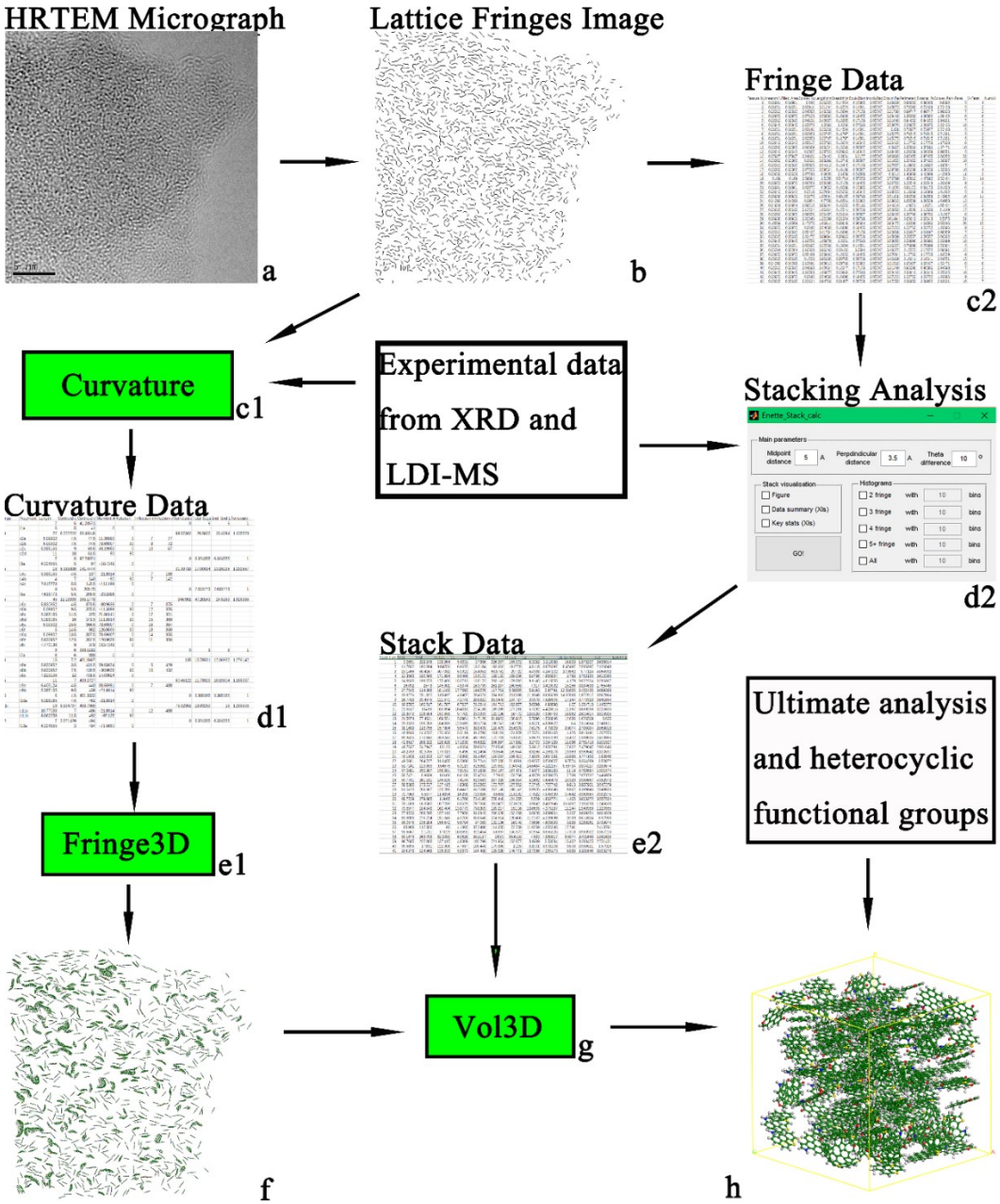

Figure 1. Schematic diagram of the HRTEM analytic technique.

Digital Micrograph (DM) is a free software tool widely used for preprocessing HRTEM images in materials science. It enables image enhancement and noise reduction, facilitating subsequent analysis. The typical preprocessing workflow includes contrast adjustment, Fast Fourier Transform (FFT), lattice region calibration, and Inverse Fourier Transform (IFFT), resulting in a clearer image with reduced background noise. These enhanced images are then subjected to binarization to extract lattice fringes.

The HRTEM analysis software combines Adobe Photoshop with the FoveaPro plugin, a professional image processing tool originally developed for use within Photoshop. While binarization is just one application of FoveaPro, the integration allows for a semi-automated workflow (as shown in the right-hand panel of the software interface), enabling fast and precise tracing of lattice fringes. The software also offers analytical functions, categorizing lattice fringes by extension direction (angle) and length using distinct color coding.

The orientation of the lattice fringes was quantified using the distribution of fringe angles and fringe contribution within a 15° angle bin (divide 180° into twelve 15° angle bins) to total fringes. Each image was rotated until the largest proportion of fringes was concentrated between 60° and 105° (45° contribution), allowing the comparison at different temperature stages.

Two Matlab-based tools, Stack and Curvature, were employed for further structural analysis. The Stack software determines whether two or more lattice fringes are stacked based on three criteria: the angle between fringes, the center-to-center distance, and the perpendicular distance from one fringe to the center of another. Given the interlayer spacing of graphite (~3.5 Å), fringe pairs with an angle < 20°, center distance < 5 Å, and perpendicular distance < 4 Å are considered stacked. This rule is extended to define multi-layer stacking (e.g., two, three, four, or five layers). The average stacking order was calculated by summing the frequencies multiplied by the corresponding layers of the four types of stacking. The Curvature script models bent lattice fringes by segmenting them into small linear sections. It calculates segment length, coordinates, bending angle, and cumulative curvature. The minimum segment length and minimum inter-segment angle are user-defined parameters that control the resolution and accuracy of curvature detection. Starting from a fringe's origin, the script proceeds according to these rules to capture its structural geometry.

Fringe3D is a Perl-based modeling script executed within the Cygwin64 Terminal emulator. It defines key modeling rules and arrangements, serving as one of the core components in HRTEM-based automatic structural modeling. Fringe3D adopts a circular ring arrangement model. Each benzene ring is assumed to correspond to a fringe of approximately 3 Å. Lattice fringes shorter than 3 Å are excluded from analysis, as they are unlikely to represent aromatic structures. In this model, lattice fringes are idealized as having similar length and width. For example, a 10 Å fringe is treated as an aromatic sheet with roughly 35–40 carbon atoms. Longer fringes indicate larger sheets with more atoms. The script draws aromatic layers of various shapes and sizes based on fringe length and aligns them spatially using fringe coordinate and orientation data. This allows the generation of realistic, spatially resolved molecular representations of the carbon structure.

2.3 Additional Characterization

X-ray Diffraction (XRD) patterns of the samples were collected on the Rigaku diffractometer (Rigaku TTR-III, Cu-Kα radiation, λ = 1.54 Å, tube voltage = 40 kV, electric current = 250 mA). Based on the XRD spectra, the radial distribution function ($g(r)$) can be analyzed, which is defined as shown in Equation 1. Fourier Transform Infrared Spectroscopy (FT-IR) measurement was performed using Nicolet iS50 FT-IR spectrometer manufactured (Thermo, USA) to analyze the aromaticity (f_a), which is defined as shown in Equation 2. X-ray Photoelectron Spectroscopy (XPS) spectra was generated using ESCALAB250 X-ray photoelectron spectrometer (Alka anode with

200 W, pass energy = 60 eV, energy step size = 0.05 eV) to determine the content of ONS functional groups. Based on the XPS spectra, The functional group types were determined by the peak position of the fitted curves, and the proportion of functional groups were determined by the area ratio of related peaks.

$$g(r) = 4\pi r^2[\rho(r) - \rho_0] \quad (1)$$

where:
$g(r)$ The radial distribution function
$\rho(r)$ The microscopic pair density
ρ_0 The average number density
r The interatomic distance, Å

$$f_a = 1 - I_{al}/(I_{ar}+I_{al})\times(H/C)\times(C_{al}/H_{al}) \quad (2)$$

where:
f_a The aromaticity
I_{ar} The aromatic related absorption-peak density
I_{al} The aliphatic related absorption-peak density
H/C The atom ratio of hydrogen to carbon
C_{al}/H_{al} The atom ratio of carbon to hydrogen on aliphatic chains

3. Results and Discussion

3.1 Microstructural Representation of GPC

The structural characteristics of lattice fringes (aromatic layers) within petroleum coke were statistically analyzed using high-resolution transmission electron microscopy (HRTEM), as summarized in Figure 2a. The results indicate that 10 to 25 % of the lattice fringes are approximately 5 Å in length, with another significant concentration in the 10–15 Å range. Overall, more than 90 % of the total fringe length is composed of fringes shorter than 15 Å, while fringes longer than 20 Å are extremely rare. Analysis of fringe orientation reveals that directions within 45° account for 22.7% more than a random distribution, indicating a moderate degree of directional ordering. The average stacking order derived from HRTEM analysis ranges from 2.05 to 2.16, with a mean value of 2.11, suggesting a relatively low degree of stacking order. Furthermore, based on the proportion of total fringe length, 62.2 % of the lattice fringes are non-linear, reflecting substantial curvature and disorder. Collectively, these results demonstrate that petroleum coke exhibits a highly disordered carbon atomic arrangement at the microscopic level. When compared to coal structures, its structural maturity lies between that of low-rank and medium-rank coals.

The construction of the coke molecular models was performed in four systematic steps to ensure both structural and compositional rationality. First, the lengths of individual lattice fringes were extracted from HRTEM images. Each lattice fringe was then converted into a corresponding aromatic layer based on the Fringe3D script and established growth rules of aromatic structures, resulting in a library of aromatic layers with diverse sizes and geometries. Second, 3D models were assembled by selecting aromatic layers from the library according to the statistical distributions of fringe lengths, orientations, and stacking proportions observed in the HRTEM analysis. This procedure guarantees that the overall structural features of the models reflect the microstructural characteristics of the coke samples. In the third step, the compositional details were incorporated. Guided by elemental analysis, XPS, and FT-IR data (Table 2 “Actual” column), a customized script was employed to automatically add hydrogen atoms, aliphatic

carbons, and heteroatom-containing functional groups to the selected aromatic layers. This ensured that the resulting models were chemically representative of the coke materials. Finally, the assembled molecular models were subjected to multi-level validation, including comparisons with experimental observations, to confirm their reliability in capturing the structural and compositional characteristics of the materials.

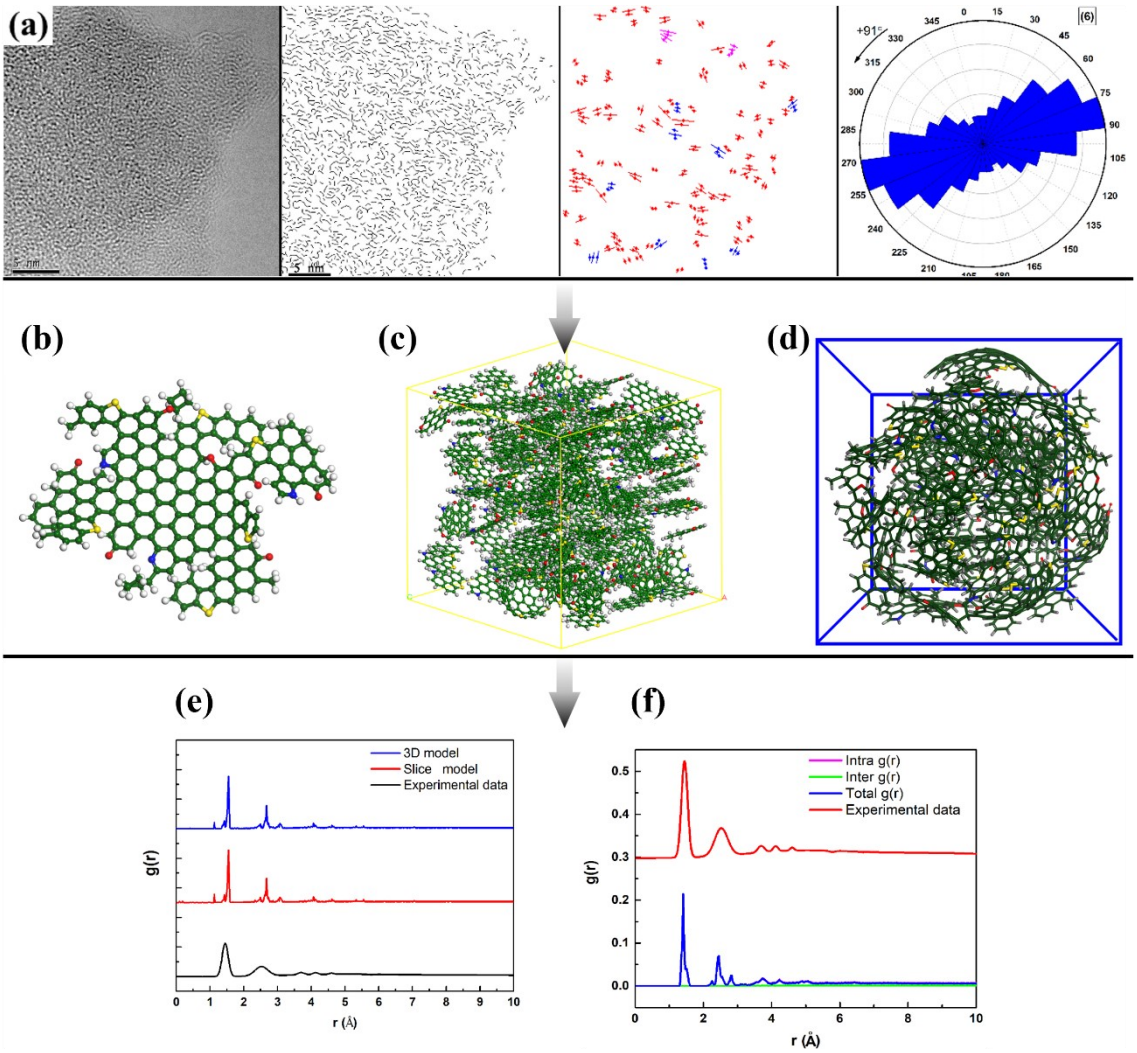

Figure 2. (a): The microstructural analysis for GPC based on HRTEM, (b): molecular model, (c): 3D lattice model, (d): particle model of GPC (green for carbon, red for oxygen, yellow for sulfur, blue for nitrogen, and grey for hydrogen), and (e)(f): the PDF verification for the models.

Based on the flow above, three types of structural models were constructed using petroleum coke as a template: a single-molecule model (GPC 1), a 3D lattice model (GPC 2), and a particle model (GPC 3). GPC 1 (Figure 2b) illustrates the types and relative proportions of carbon structures and O/N/S functional groups at a fine scale. GPC 2 (Figure 2c) provides a stereoscopic representation of the internal structure of petroleum coke, useful for studies on adsorption, reactivity, and gasification. To enable ReaxFF simulations, which require a fully connected molecular framework to accurately describe reactive processes, GPC 3 (Figure 2d) was constructed using cross-linking. The cross-linking sites were selected as aliphatic carbon atoms located at the periphery of aromatic layers. Using a customized script, pairs of aliphatic carbons from adjacent layers were automatically identified. The script then removed the hydrogen atoms attached to these carbons and created covalent bonds between them, effectively linking the aromatic layers

into a single three-dimensional network. A comparison between the composition of the constructed GPC models and experimental data is shown in Table 2. Owing to the large model size and high-fidelity simulation methods, the model values closely match the experimental values across key metrics. To further evaluate the structural validity of the model, the radial distribution function *g(r)* was calculated. All model-generated *g(r)* curves exhibit strong peaks at approximately 1.5 Å and 2.7 Å, consistent with the experimental *g(r)* data. This confirms the overall structural rationality of the constructed models.

Table 2. The comparison between the components of the created GPC models and the actual sample.

	Actual	GPC 1	GPC 2	GPC 3
C (atom %)	63.94	63.79	63.60	64.63
H (atom %)	30.86	30.90	31.31	30.28
Ether (atom %)	0.80	0.78	0.75	0.79
Carbonyl (atom %)	1.56	1.55	1.53	1.52
Pyrrole (atom %)	0.64	0.66	0.62	0.62
Pyridine (atom %)	0.33	0.34	0.31	0.32
Thiophene (atom %)	1.87	1.99	1.86	1.84
f_a (aromaticity)	0.79	0.79	0.79	0.80

3.2 Microstructural Representation of CPC

Above 1673 K, the structural transformation of calcined petroleum coke (CPC) is essentially complete, and this temperature aligns well with typical industrial calcination conditions. Therefore, CPC calcined at 1673 K was selected for detailed microscopic structural analysis and multiscale model construction. The HRTEM analysis (Figure 3a) revealed that the average lattice fringe length of the CPC is 11.69 Å. The stacking ratio is 50.26 %, and 97.54 % of the fringes are oriented within 45°, indicating a high degree of directional ordering. Additionally, 36.27 % of the fringes are curved, reflecting a moderate level of structural distortion.

Based on these data, three structural models of CPC (Figure 3b-d) were constructed at different scales: a molecular-scale model (~70 atoms, CPC1, including the planar and cambered molecule models), a 3D lattice model (3 990 atoms, CPC 2), and a nanoscale 3D model (31 909 atoms, CPC3). These models exhibit realistic values in terms of H/C ratio, functional group distribution, and structural features, closely matching the corresponding experimental data.

Density functional theory (DFT) was employed to obtain the FT-IR spectrum of the molecular model. The ratio of peak areas corresponding to aromatic (from 2800 to 3100 cm^{-1}) and aliphatic (from 2800 to 3100 cm^{-1}) hydrogen was used to calculate the *fa* of the model, which presented good consistency with the experimental measurements in both peak positions and f_a values. Additionally, XRD patterns were simulated for the 3D models using custom scripts. The resulting diffraction peaks closely match those obtained from experimental data, further validating the structural accuracy of the models. Overall, the multiscale models developed in this study provide an accurate and comprehensive representation of the microstructure of CPC calcined at 1673 K, supporting their application in further theoretical and simulation-based investigations.

Table 3. The comparison between the components of the created CPC models and the actual sample.

	Actual	CPC 1	CPC 2	CPC 3
C (atom%)	88.78	88.69	88.78	88.78
H (atom%)	8.75	8.91	8.74	8.74
Ether (atom %)	1.00	0.98	1.00	1.00
Carbonyl (atom %)	0.48	0.44	0.47	0.47
Pyrrole (atom %)	0.05	0.03	0.04	0.04
Pyridine (atom %)	0.30	0.32	0.5	0.6
Thiophene (atom %)	0.65	0.63	0.66	0.66
f_a (aromaticity)	0.98	0.96	0.98	0.98

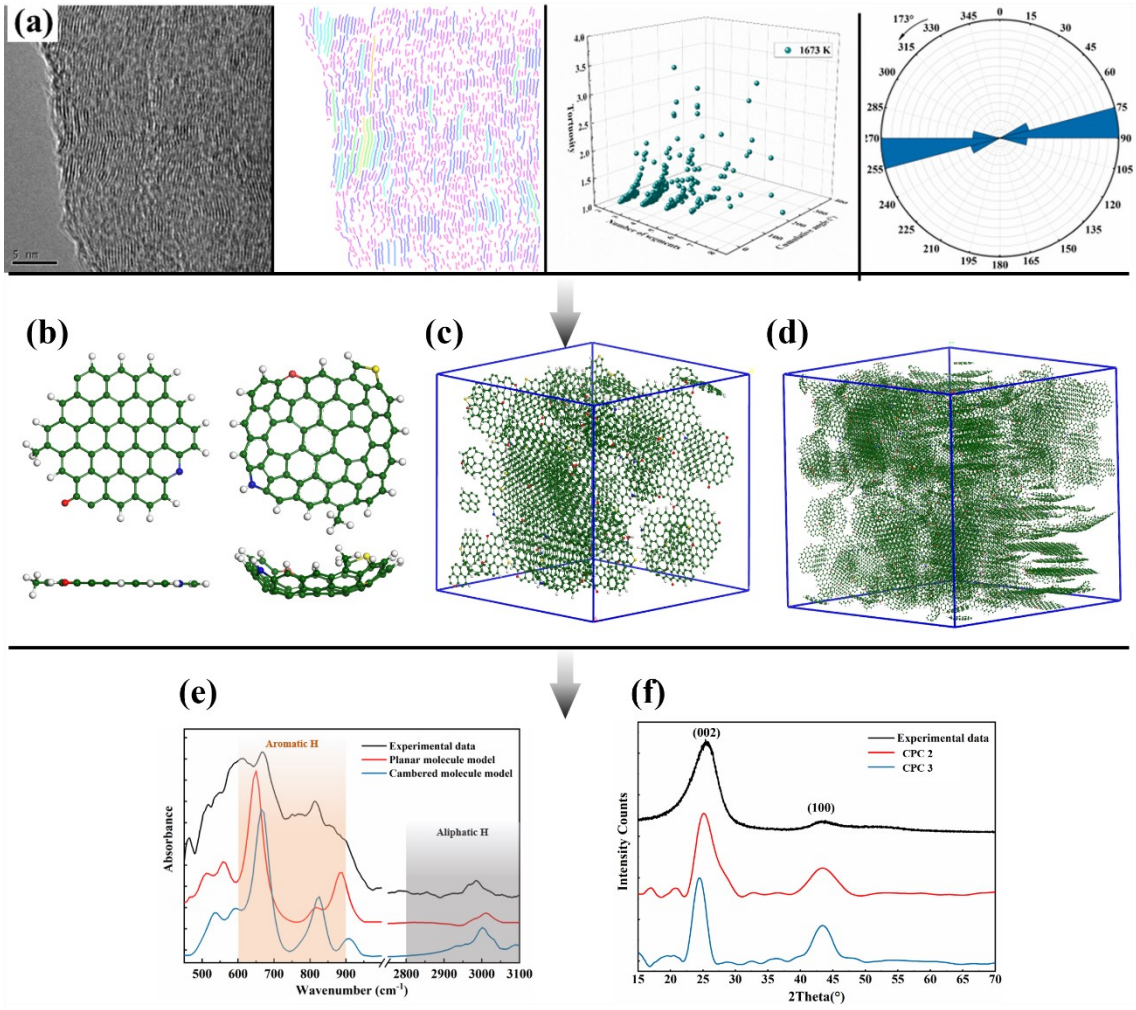

Figure 3. (a) The microstructural analysis for CPC based on HRTEM, (b) CPC 1 model (left is the planar molecule model and right is the cambered molecule model), (c) CPC 2 model, (d) CPC 3 model (green for carbon, red for oxygen, yellow for sulfur, blue for nitrogen, and grey for hydrogen), and (e)-(f) the DFT verification for the models.

3.3 Microstructural Transformation of PC

Figure 4 illustrates the lattice fringe micrographs extracted from HRTEM images of PC samples calcined at different temperatures. These micrographs reveal the temperature-dependent growth behavior of lattice fringes. In the low-temperature range of (298-873) K, fringe development is minimal, and the overall structure exhibits an amorphous character with a disordered atomic arrangement. At 1073 K, longer fringes begin to emerge at the particle edges, indicating that aromatic molecules start to grow from the surface during calcination. As the temperature increases from 1073 K to 1873 K, the fringe length progressively increases, the overall structure becomes increasingly ordered, and the features of graphitic microcrystals become more apparent.

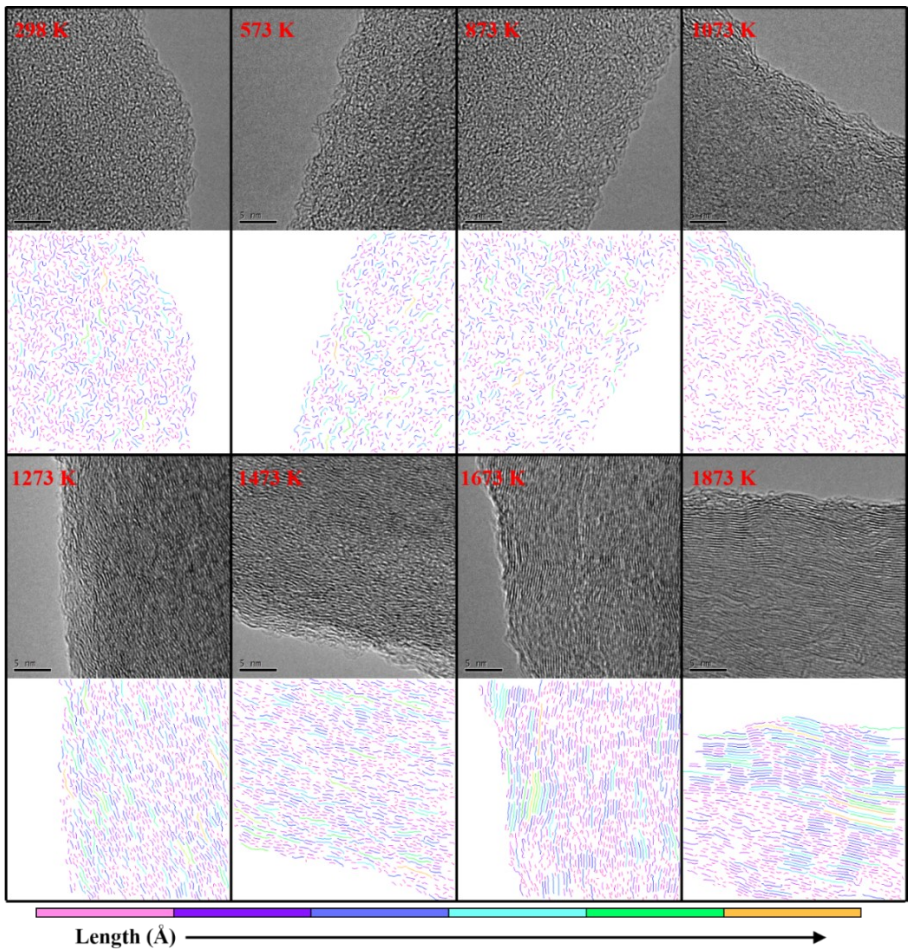

Figure 4. The HRTEM micrographs of PC at multiple temperature stages (above) and corresponding lattice fringe micrographs (below).

To investigate the structural evolution trends, key microstructural parameters of PC calcined at various temperatures were quantitatively fitted, as shown in Figure 5. The average fringe length (L_T, Figure 5a) slightly decreases below 873 K, followed by a sharp increase above 873 K, reaching a maximum of 12.03 Å at high temperature. The stacking configuration of calcined coke comprises two-layer, three-layer, four-layer, and five-layer stacking types. The sum of the four stacking types constitutes the total stacking frequency (S_T, Figure 5b), which decreases initially and then increases with temperature, ranging from 10.26 to 50.63 %. These results suggest that at lower temperatures, activation of growth sites can induce slight disruption to the lattice structure. However, above 1073 K, graphite-like microcrystals grow rapidly, enhancing the overall structural ordering of the calcined coke.

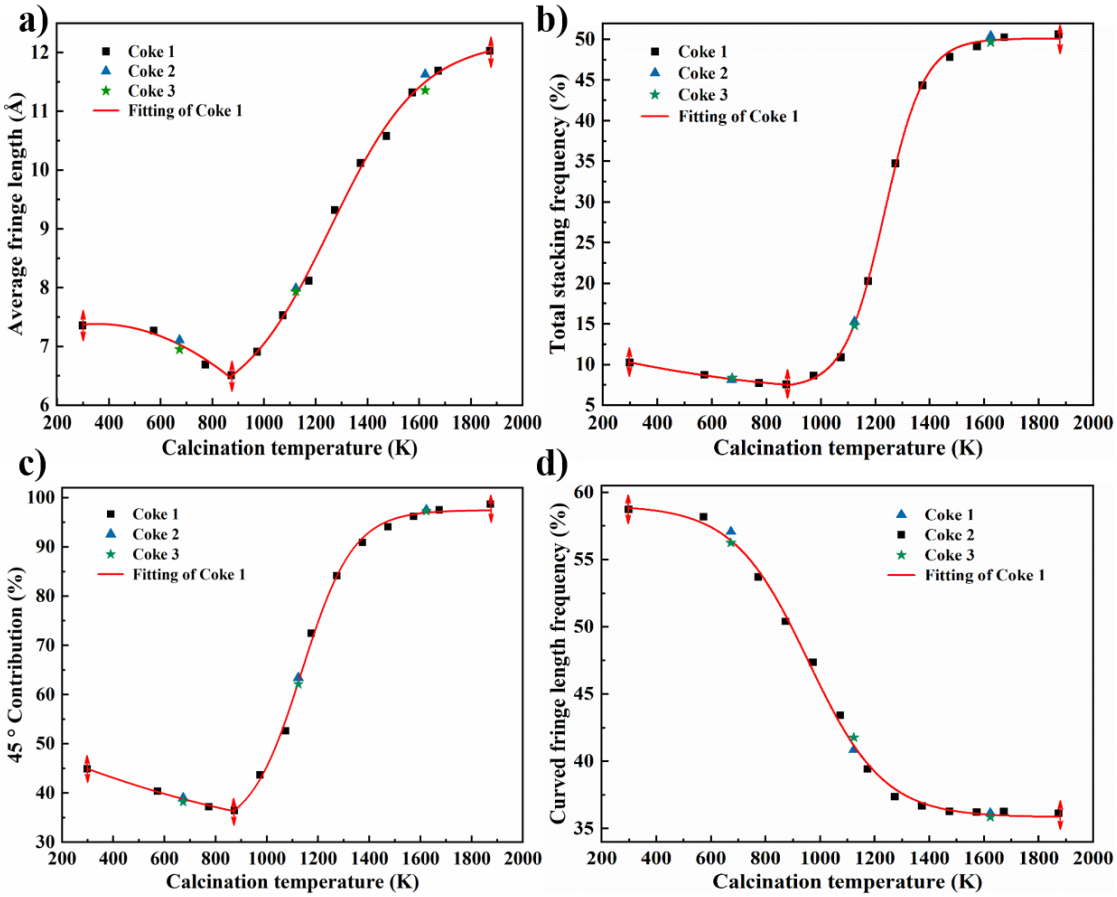

Figure 5. The curve fitting and verification of (a) average fringe length, (b) total stacking frequency, (c) 45-degree contribution, and (d) curved fringe length frequency of PC at different temperature stages.

To quantify lattice fringe orientation, fringe images were rotated such that the majority of fringe directions fell within a 45° angular range. The maximum proportion of fringes within this range is defined as the 45-degree contribution (A_T, Figure 5c). The A_T value exhibits a slow decline followed by a sharp increase with temperature and eventually stabilizes. At 1873 K, A_T reaches a maximum of 98.71 %, significantly higher than that of raw petroleum coke but still lower than that of graphite, indicating that high-temperature calcined petroleum coke possesses a moderate degree of structural order and can be classified as a graphitization intermediate.

Curved lattice fringes originate from defects in the carbon layers. Their curvature characteristics are quantified by the cumulative bending angle, number of segments, and curvature values. The curved fringe length frequency (C_T) decreases with increasing temperature in a sigmoidal trend – slow at first, then rapidly, and eventually leveling off.

In the temperature range of 873–1873 K, the evolution of microstructural features fits well with Logistic Regression models ($y = 1 / (1 + e^{-x})$), the results are exhibited in Figure 5. The corresponding mathematical expressions are given in Equations (1–4), where T refers to the calcination temperature. These equations can be used to predict microstructural parameters of calcined coke at a given temperature. When applied to verify two additional coke samples, Coke 2 and Coke 3, calcined at 673 K, 1123 K, and 1663 K, the calculated values using Equations (3–6) showed a deviation of less than 2 % from the experimental results (Table 4), demonstrating the high accuracy and predictive power of the proposed models.

$$L_T = 5.8458 + \frac{6.3705}{1 + e^{-0.0057\cdot(T-1257.8528)}} \quad 873\ K \le T \le 1873\ K \quad (3)$$

$$S_T = 7.1185 + \frac{42.9861}{1 + e^{-0.0136\cdot(T-1233.007)}} \quad 873\ K \le T \le 1873\ K \quad (4)$$

$$A_T = 32.0327 + \frac{65.4622}{1 + e^{-0.0099\cdot(T-1136.504)}} \quad 873\ K \le T \le 1873\ K \quad (5)$$

$$C_T = 59.0331 - \frac{23.1935}{1 + e^{-0.0073\cdot(T-956.933)}} \quad 298\ K \le T \le 1873\ K \quad (6)$$

where:

T	Temperature, K
L_T	Average fringe length, Å
S_T	Total stacking frequency, %
A_T	45-degree contribution, %
C_T	Curved fringe length frequency, %

Table 4. The comparison of the deductive and actual value of the microstructural features

Calcining temperature (K)		673	1123	1623
L_T	Deductive value (Å)	7.03	7.87	11.50
	Actual value of Coke 2 (Å)	7.11	7.99	11.63
	Actual value of Coke 3 (Å)	6.95	7.94	11.36
	Maximal error	1.21 %	1.50 %	1.23 %
S_T	Deductive value (%)	8.22	14.98	49.89
	Actual value of Coke 2 (%)	8.15	15.27	50.41
	Actual value of Coke 3 (%)	8.36	14.82	49.67
	Maximal error	1.67 %	1.89 %	1.03 %
A_T	Deductive value (%)	38.79	62.55	96.95
	Actual value of Coke 2 (%)	38.98	63.41	97.50
	Actual value of Coke 3 (%)	38.21	62.13	97.31
	Maximal error	1.52 %	1.36 %	0.56 %
C_T	Deductive value (%)	56.42	41.18	36.02
	Actual value of Coke 2 (%)	57.08	40.86	36.15
	Actual value of Coke 3 (%)	56.25	41.77	35.86
	Maximal error	1.16	0.78	1.41

4. Conclusions

This work presents an HRTEM analytic technique for the intelligent extraction and analysis of lattice fringes in carbon materials, developed through the integration of HRTEM imaging, binary image processing techniques, and customized Matlab and Perl scripts. The developed technique enables quantitative analysis of lattice fringe characteristics such as length, stacking, orientation, and curvature. It fills a critical gap in the precise structural analysis of aluminum electrolysis carbon materials and applies to a broad range of studies on the microstructural evolution of various carbon-based materials.

Representative models of PC were constructed at the molecular scale, 3D microcrystalline scale, and 3D nanoscale. The DFT calculations were used to generate FT-IR and XRD spectra, which confirm the aromaticity and degree of ordering in the constructed models. For the three coke materials tested, the multi-level validation affirms the accuracy and reliability of the models. Beyond visualizing the microstructure of calcined coke, these models also provide a robust platform for quantitative simulations and molecular dynamics studies of various reactive processes in metallurgical carbon materials.

The HRTEM analytical technique, in combination with mathematical fitting, was employed to continuously and quantitatively evaluate the evolution of PC microstructures as a function of calcination temperature. In the temperature range of 873–1873 K, the microstructural parameters exhibit excellent agreement with Logistic regression models. Below 873 K, the structure undergoes slight disordering, while above this threshold, a significant increase in structural ordering is observed. Mathematical equations derived from the fitted curves enabled the reliable prediction of key microstructural features of the three tested coke samples at any given temperature.

5. Acknowledgements

This work was supported by the National Natural Science Foundation of China (NO. 52174338, 52374421, and 52404318), the Science and Technology Innovation Program of Hunan Province (2024RC3039), Young Elite Scientists Sponsorship Program by CAST, China (No.YESS20210258), Program of China Scholarships Council (No. 202406370261), Central South University Innovation-Driven Research Programme (No.2023CXQD005), Education Department of Hunan Provincial Government (23B0841), Yunnan Province Science and Technology Planning Project No.202202AB080017, and Guizhou Provincial Science and Technology Projects No.[2023]General212. This work was supported in part by the High-Performance Computing Center of Central South University, the National Engineering Research Centre of Low-carbon Nonferrous Metallurgy, and the XIAOMI Foundation.

6. References

1. M. Wissler, Graphite and carbon powders for electrochemical applications, *Journal of Power Sources*, Vol. 156, No. 2, (2006), 142–50. https://doi.org/10.1016/j.jpowsour.2006.02.064.
2. Xiao Jin et al., Modelling the Change of Green Coke to Calcined Coke Using Qingdao High-Sulfur Petroleum Coke*, Energy & Fuels*, Vol. 29, No. 5, (2015), 3345–52. https://doi.org/10.1021/acs.energyfuels.5b00021.
3. Jonathan P. Mathews et al., Determining the molecular weight distribution of Pocahontas No. 3 low-volatile bituminous coal utilizing HRTEM and laser desorption ionization mass spectra data, *Fuel*, Vol. 89, No. 7, (2010), 1461-69. https://doi.org/10.1016/j.fuel.2009.10.014.

4. Jonathan P. Mathews, Adri Van Duin and Alan L. Chaffee, The utility of coal molecular models, *Fuel Processing Technology*, Vol. 92, No. 4, (2011), 718–-28. https://doi.org/https://doi.org/10.1016/j.fuproc.2010.05.037.
5. Jonathan P. Mathews and Atul Sharma, The structural alignment of coal and the analogous case of Argonne Upper Freeport coal, *Fuel*, Vol. 95, No. 1, (2012), 19–24. https://doi.org/10.1016/j.fuel.2011.12.046.
6. Enette B. Louw, Structure and combustion reactivity of inertinite-rich and vitrinite-rich South African coal chars: quantification of the structural factors contributing to reactivity differences. *The Pennsylvania State University*; 2013.
7. Enette B. Louw et al., Constitution of Drop-Tube-Generated Coal Chars from Vitrinite- and Inertinite-Rich South African Coals, *Energy & Fuels*, Vol. 30, No. 1, (2016), 112-20. https://doi.org/10.1021/acs.energyfuels.5b01517.
8. Chang'an Wang et al., Quantifying Curvature in High-Resolution Transmission Electron Microscopy Lattice Fringe Micrographs of Coals, *Energy & Fuels*, Vol. 30, No. 4, (2016), 2694–704. https://doi.org/10.1021/acs.energyfuels.5b02907.
9. Huang Yang et al., Activated carbon efficient atomistic model construction that depicts experimentally-determined characteristics, *Carbon*, Vol. 83, No. (2015), 1–14. https://doi.org/10.1016/j.carbon.2014.11.012.
10. Leandro Martinez et al., PACKMOL: A Package for Building Initial Configurations for Molecular Dynamics Simulations, *Journal of Computational Chemistry*, Vol. 30, No. 13, (2009), 2157–64. https://doi.org/10.1002/jcc.21224.